On the solute dispersion in a pipe of annular cross-section with absorption boundary

Kajal Kumar Mondal and Bijoy S. Mazumder*

Physics and Applied Mathematics Unit, Indian Statistical Institute, Calcutta 700 108, India

The paper presents the longitudinal dispersion of passive tracer molecules released in a steady laminar flow through an annular pipe with heterogeneous reaction at the outer wall, which causes a depletion of contaminant in the flow. A finite-difference implicit scheme has been adopted to solve the unsteady advection-diffusion equation for all time period. Here, it is shown how the spreading of tracers is influenced by the shear flow, the aspect ratio (the ratio of the inner radius to the outer radius of the annular pipe), and the absorption parameter at the outer wall. The solute disperses in the annular region due to the interaction between advection and transverse diffusion. Three stages of longitudinal dispersion with time, named as diffusive regime, anomalous regime, and Taylor's regime observed for Poiseuille flow, are discussed for an annular pipe with absorption boundary. The axial distributions of mean concentration are determined from the first four central moments using Hermite polynomial representation. The results of this study are likely to be of interest for understanding the interaction between flow and dispersion in a catheterized artery with conductive walls.

1 Introduction

The study of longitudinal dispersion of a tracer in a straight tube has a wide range of applications in the field of chemical and environmental engineering, biomedical engineering, and physiological fluid dynamics. The dispersion of a diffusing solute in a fluid flowing through a circular impermeable tube, relative to a plane moving with the mean speed of the flow, was first studied by Taylor [1]. Aris [2] generalized Taylor's conceptual model by removing restrictions made by Taylor to include longitudinal diffusion, and proposed the idea of moment method to analyze the asymptotic nature of the second moment about the mean. Both authors noted that after a sufficiently large time when the tracer is mixed completely across the tube, the shape of the distribution of the tracer material evolves to a Gaussian distribution. Lighthill [3] presented an exact solution for the advection-diffusion equation incorporating the transverse diffusion, neglecting the longitudinal diffusion and interaction with the boundary of the pipe. However, his solution was asymptotically valid for small time. Chatwin [4] developed an asymptotic series solution for the distribution of concentration and showed that his solution for the mean concentration approached to Gaussian form at large time. Gill and Sankarasubramanian [5] presented an exact analysis of unsteady convective diffusion in a fully developed laminar flow through an impermeable tube. They showed that the solution of the advection-diffusion equation with a time-dependent dispersion coefficient can be obtained using the series expansion method. Sankarasubramanian and Gill [6], and Rao and Deshikachar [7] used the generalized dispersion model proposed by Gill and Sankarasubramanian [5] to study the dispersion of a diffusing substance in an annular pipe and evaluated the dispersion coefficient for all time period. A modification to the Taylor dispersion theory with an asymptotic expansion similar to Chatwin's model for the classical theory has been developed by Frankel and Brenner [8]. Stokes and Barton [9] studied the shear dispersion in a tube based on Laplace and Fourier transforms, which led to an eigenvalue problem. Since the pioneering work of Taylor [1], dispersion problems have been extensively studied to cover a great variety of transport problems, but dispersion with absorption at the boundary has received little attention.

Gupta and Gupta [10] studied the dispersion of a reactive solute in a liquid flowing through a channel in presence of a first order heterogeneous reaction using Taylor's conceptual asymptotic model for large time. Smith [11] used a delay-diffusion equation to study the effect of the boundary reaction on the longitudinal dispersion in shear flows. Barton [12] explained the dispersion of a reactive solute in Poiseuille flow in the presence of a boundary reaction for large time and presented the results for the concentration distribution for weak and vigorous reactions at the boundary. Mazumder and Das [13]

studied the effect of wall conductance on the axial dispersion in the pulsatile flow through a tube. Using a numerical scheme, they computed the dispersion coefficient for different values of absorption parameter, which are valid for all time period. Jayaraman et al. [14] studied the dispersion of a solute in a fluid flowing through a curved tube with absorbing walls. Their results basing on perturbation and spectral methods confirmed that the influence of secondary flows on the dispersion was reduced if the tracer was heavily soluble in the wall. Sarkar and Jayaraman [15] studied the effect of wall absorption in annular flows based on the generalized dispersion model proposed by Gill and Sankarasubramanian [5].

Latini and Bernoff [16] presented a new solution based on the Fourier transformation for the advection-diffusion equation valid for the time before the existence of the Taylor regime. They showed that the tracer dispersion in a pipe can be divided into three regimes: The initial diffusive regime which is valid for a small time period ($t_{LB} \leq D^{-1/3}$) yielding a Gaussian distribution of the solute; the anomalous regime for an intermediate time period ($D^{-1/3} \leq t_{LB} \leq D^{-1}$), where the distribution is clearly asymmetric and is convected with the centerline velocity in the pipe; and the Taylor's regime for a large time period ($t_{LB} \geq D^{-1}$), where the concentration distribution is again a Gaussian distribution. They defined the dimensionless diffusion coefficient D as the inverse of the Péclet number Pe, and t_{LB} corresponds to the time. However, their method of solution is restricted only to locally quadratic or linear shear flow. The Taylor's regime of dispersion has received much attention in the literature.

The main objective of the present paper is to study the combined effect of the boundary absorption or the first-order heterogeneous chemical reaction at the outer wall and the aspect ratio on the stream-wise dispersion of a solute released in a steady laminar flow through an annular pipe. More precisely, results are shown for all time period describing how the spreading of tracers is influenced by the shear flow, the reaction parameter and the aspect ratio, how the center of mass moves, and what the pattern of the mean concentration distributions in three different dispersion regimes is. A numerical scheme (Crank-Nicholson implicit type) has been adopted to solve the advection-diffusion equation for all time periods when the solute is injected uniformly over the cross-section of the annular pipe. The mean concentration distribution is approximated by an Edgeworth series expansion using the first four central moments. The recent interest in the analysis of shear dispersion in presence of boundary absorption has been motivated by deposition, chemical reaction, and the dispersion of tracers in blood flow in an annular region. The insertion of a catheter into an artery leads to a formation of an annular region between the catheter and the artery wall, which brings an additional impedance or frictional resistance to the flow and therefore alters the pressure and velocity distributions. Since the lung and blood vessels have conductive walls, it is important to analyze the dispersion phenomena in presence of conductive walls to understand the indicator technique and other mechanisms in the bronchial region.

2 Mathematical formulation

A steady, fully developed, viscous, incompressible, axi-symmetric, laminar, two-dimensional flow under the action of a constant pressure gradient P is considered in an annular pipe along the z^*-axis (Fig. 1). The fluid flow in the annular pipe can be described by the continuity and the Navier-Stokes equations together with no-slip boundary conditions at the walls. The velocity component in the axial direction in the polar coordinates (r^*, z^*) is given by Bird et al. [17] as:

$$u^* = u_0 \left[1 - \frac{r^{*2}}{a^2} - \frac{1 - \lambda^2}{\log \lambda} \log \frac{r^*}{a} \right], \quad 0 < \lambda < 1, \tag{1}$$

where $u_0 = \frac{Pa^2}{4\mu}$, $\lambda = \frac{b}{a}$ is the ratio of the inner radius b to the outer radius a of the annular pipe, and μ is the viscosity of the fluid. As $\lambda \to 0$, eq. (1) corresponds to the pipe Poiseuille flow $u^* = u_0(1 - \frac{r^{*2}}{a^2})$, which leads to the maximum velocity at the center line of the pipe $r^* = 0$. Fig. 2 shows the velocity profiles for various aspect ratios λ. The insertion of a pipe with smaller diameter at the center line of an artery brings the asymmetry to the flow, and the increase of aspect ratio λ leads to the existence of symmetry of the annular flow. Here, the blood may be assumed to be a homogeneous, incompressible,
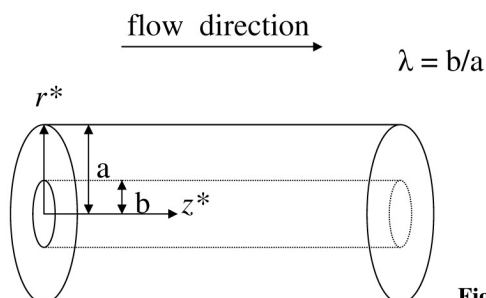

Fig. 1   Schematic diagram of an annular pipe.

Newtonian fluid and the oxygen is used as a passive solute. When the passive solute is released in the above mentioned flow in an annular pipe with absorption at the outer wall, the concentration $C(t, r, z)$ of the reactive solute with constant molecular diffusivity D satisfies the non-dimensional advective-diffusion equation of the form

$$\frac{\partial C}{\partial t} + \text{Pe}\, u(r) \frac{\partial C}{\partial z} = \frac{1}{r} \frac{\partial}{\partial r} \left(r \frac{\partial C}{\partial r} \right) + \frac{\partial^2 C}{\partial z^2}, \tag{2}$$

where the dimensionless quantities are

$$r = \frac{r^*}{a}, \quad z = \frac{z^*}{a}, \quad t = \frac{Dt^*}{a^2}, \quad u = \frac{u^*}{u_0}, \quad \text{Pe} = \frac{u_0 a}{D}.$$

Here, Pe is the Péclet number which measures the relative characteristic time of the diffusion process $\left(\frac{a^2}{D} \right)$ to that of the convection process $\left(\frac{a}{u_0} \right)$. The Péclet number Pe is very large in typical applications (blood flow, sewage dispersion etc.) as the molecular diffusion coefficient is quite small. The initial and boundary conditions are

$$\left.\begin{array}{l}
C(0, r, z) = B(r)\delta(z), \quad (\lambda \leq r \leq 1), \\[2mm]
\dfrac{\partial C}{\partial r} + \beta C = 0 \quad \text{at} \quad r = 1, \quad \text{at the outer wall of the annular pipe}, \\[2mm]
\dfrac{\partial C}{\partial r} = 0 \quad \text{at} \quad r = \lambda, \quad \text{at the inner wall of the annular pipe}, \\[2mm]
C \quad \text{finite at all points}, \\[2mm]
z^n C \quad \text{and} \quad z^m \dfrac{\partial^n C}{\partial z^n} \to 0 \quad \text{as} \quad |z| \to \infty \quad \text{for} \quad m, n = 0, 1, 2, \dots, \\[2mm]
\dfrac{1}{1-\lambda} \dfrac{1}{\pi} \displaystyle\int_\lambda^1 \int_0^{2\pi} \int_{-\infty}^\infty r C(0, r, z) dr d\theta dz = 1,
\end{array}\right\} \tag{3}$$

where $B(r)$ is a function of r, $\delta(z)$ is the Dirac delta function and $\beta \, (= \beta^* a)$ is the first order reaction rate or absorption parameter. The last condition of eq. (3) represents the total amount of material at the annular pipe is unity.

Following the Aris [2] method of moments, the p-th integral moment of the concentration distribution can be defined as

$$C_p(t, r) = \int_{-\infty}^{+\infty} z^p C(t, r, z) dz \tag{4}$$

and the concentration distribution of the tracer over the cross-section of the annulus is

$$M_p(t) = \bar{C}_p = \frac{\int_0^{2\pi} d\theta \int_\lambda^1 r C_p(t, r) dr}{\int_0^{2\pi} d\theta \int_\lambda^1 r dr}. \tag{5}$$

Hence, using (4) and (5), the diffusion eq. (2) with respective initial and boundary conditions becomes

$$\frac{\partial C_p}{\partial t} - \frac{1}{r} \frac{\partial}{\partial r} \left(r \frac{\partial C_p}{\partial r} \right) = p u(r) \text{Pe}\, C_{p-1} + p(p-1) C_{p-2} \tag{6}$$

with

$$C_p(0, r) = \begin{cases} B(r) & \text{for} \quad p = 0, \\ 0 & \text{for} \quad p > 0, \end{cases} \tag{7}$$

$$\frac{\partial C_p}{\partial r} + \beta C_p = 0 \quad \text{at} \quad r = 1, \tag{8}$$

$$\frac{\partial C_p}{\partial r} = 0 \quad \text{at} \quad r = \lambda, \tag{9}$$

where $B(r) = 1$ for $\lambda \leq r \leq 1$ and

$$\frac{dM_p}{dt} = p\, \text{Pe}\, \overline{u(r) C_{p-1}} + p(p-1) \overline{C_{p-2}} - \frac{2\beta}{1 - \lambda^2} C_p(t, 1) \tag{10}$$

with

$$M_p(0) = 1 \ \text{ for } \ p = 0, \qquad M_p(0) = 0 \ \text{ for } \ p > 0. \tag{11}$$

The over-bar denotes the cross-sectional mean.

The p-th order central moment of the concentration distribution about the mean can be defined as

$$\nu_p(t) = \frac{\frac{1}{1-\lambda} \frac{1}{\pi} \int_\lambda^1 \int_0^{2\pi} \int_{-\infty}^{+\infty} r(z - z_g)^p C \, dr \, d\theta \, dz}{\int \int \int C \, dv}, \tag{12}$$

where $z_g = \frac{M_1}{M_0}$ is the centroid or first moment of the solute which determines the location of the center of gravity of the slug with mean velocity in the annular flow initially located as a source, and M_0 represents the total mass of the reactive solute in the whole volume of the annular pipe. From eq. (12) ν_2 represents the variance related to the dispersion of the tracer about the mean position, the third (ν_3) and fourth (ν_4) central moments represent the skewness and the kurtosis of the distribution of the tracer, respectively. The negative value of the skewness indicates an asymmetric profile with a tail to the left of the maximum and the large positive value of the kurtosis ($\beta_3 > 3$) indicates a profile with a much narrower peak than the Gaussian distribution.

3   Solution procedure

For $p = 0$ in (6)–(9), the equation for C_0 becomes

$$\frac{\partial C_0}{\partial t} - \frac{1}{r} \frac{\partial}{\partial r} \left(r \frac{\partial C_0}{\partial r} \right) = 0 \tag{13}$$

with the initial and boundary conditions

$$C_0(0, r) = 1, \tag{14}$$

$$\frac{\partial C_0}{\partial r} + \beta C_0 = 0 \ \text{ at } \ r = 1, \tag{15}$$

$$\frac{\partial C_0}{\partial r} = 0 \ \text{ at } \ r = \lambda, \quad 0 < \lambda < 1. \tag{16}$$

The solution of (13) with the conditions (14)–(16) is given by Carslaw and Jaeger [18]:

$$C_0(t, r) = \sum_{n=1}^{\infty} A_n E_n(\alpha_n r) e^{-\alpha_n^2 t}, \tag{17}$$

where

$$A_n = \frac{2\alpha_n^2}{[(\alpha_n^2 + \beta^2)\{E_n(\alpha_n)\}^2 - \lambda^2 \alpha_n^2 \{E_n(\alpha_n \lambda)\}^2]} \int_\lambda^1 r E_n(\alpha_n r) dr. \tag{18}$$

The α_n's are the eigen values satisfying the equation

$$\alpha_n \left[Y_1(\alpha_n \lambda) J_1(\alpha_n) - J_1(\alpha_n \lambda) Y_1(\alpha_n) \right] + \beta \left[Y_0(\alpha_n) J_1(\alpha_n \lambda) - Y_1(\alpha_n \lambda) J_0(\alpha_n) \right] = 0 \tag{19}$$

where J_0, Y_0 and J_1, Y_1 are Bessel functions of order 0 and 1, respectively. The eigen functions $E_n(\alpha_n r)$ are given by

$$E_n(\alpha_n r) = Y_0(\alpha_n r) J_1(\alpha_n \lambda) - Y_1(\alpha_n \lambda) J_0(\alpha_n r). \tag{20}$$

For $p = 1$, the first moment concentration distribution C_1 of the solute is given by

$$\frac{\partial C_1}{\partial t} - \frac{1}{r} \frac{\partial}{\partial r} \left(r \frac{\partial C_1}{\partial r} \right) = \mathrm{Pe}\, u(r) C_0. \tag{21}$$

This is a one dimensional equation having a source term $\mathrm{Pe}\, u(r) C_0$. Due to the complexity of the analytical solution of moment equations ($p \geq 1$) that are subject to the initial and boundary conditions for $\beta \neq 0$ and $\lambda \neq 0$, a finite difference

method based on a Crank-Nicholson implicit scheme has been adopted to study this problem. The scheme has been discussed in detail in the work of Mazumder and Das [13]. The derivatives and all other terms were defined at the mesh point $(i+1, j)$, where $i = 1$ corresponds to the time $t = 0$ and $j = 1$ to the inner wall of the annular pipe $r = \lambda$. The mesh point (i, j) indicates a point where $t_i = (i-1) \times \Delta t$ and $r_j = \lambda + (j-1) \times \Delta r$, Δt and Δr are the increments of t and r, respectively. The resulting finite difference equation becomes a system of linear algebraic equations with a tri-diagonal coefficient matrix

$$P_j C_p(i+1, j+1) + Q_j C_p(i+1, j) + R_j C_p(i+1, j-1) = S_j, \tag{22}$$

where P_j, Q_j, R_j, and S_j are the matrix elements.

The finite difference forms of the initial and boundary conditions are

$$C_p(1, j) = \begin{cases} 1 & \text{for } p = 0, \\ 0 & \text{for } p \geq 1, \end{cases} \tag{23}$$

$$C_p(i+1, 2) = C_p(i+1, 0) \tag{24}$$

at the inner wall of the annular pipe and

$$C_p(i+1, M+1) = C_p(i+1, M-1) - 2\beta \Delta r C_p(i+1, M) \tag{25}$$

at the outer wall of the annular pipe for $p \geq 0$. $M (= 31)$ is the value of j at the outer wall. For the steady annular flow, a mesh size of $\Delta t = 0.0001$ and $\Delta r = (1 - \lambda)/(M - 1)$ gives satisfactory results for $M = 31$. i, that corresponds to time, is ranging from 1 to N where $N_{\max} = 12000$ and j, that corresponds to annular space, is ranging from 1 to 31.

The tri-diagonal coefficient matrix was solved by the Thomas algorithm method (Anderson et al. [19]) with the help of prescribed initial and boundary conditions. The value of M_p is calculated from (10) by applying Simpson's one-third rule with the known values of $u(r)$ and C_p at the corresponding grid points. The values of the variables can be calculated iteratively for all time periods in the direction, of course.

4 Discussion of the results

In order to validate the numerical scheme, the integral moments (mean, variance and skewness) of the concentration distribution and the longitudinal dispersion coefficient for the steady flow were checked, when the aspect ratio be set to $\lambda = 0$ and absorption parameter to $\beta = 0$. The results are in good agreement with those of Gill and Sankarasubramanian [5], Barton [20], Rao and Deshikachar [7], and Mukherjee and Mazumder [21].

For $p = 0$, the eq. (10) becomes

$$M_0(t, \beta, \lambda) = 1 - \frac{2\beta}{1 - \lambda^2} \int C_0(t, 1) dt, \tag{26}$$

where $C_0(t, 1)$ is obtained from (17). Eq. (26) represents the total mass of the solute, which is a function of β, λ, and t. We observe that the total amount of the material is depleted with time. For $\beta = 0$, $M_0 = 1$ which represents a constant mass in the whole annular pipe. When β is fixed and λ increases, i.e. the annular gap decreases, the amount of slug retained in the flow decreases exponentially with dispersion time. Similar results occur for the increase of β when λ is fixed. The mean longitudinal displacement z_g of the solute moving with the mean velocity of the fluid particles mainly depends on β, λ, and the dispersion time t. It can be seen that the displacement of the center of mass (z_g) increases linearly with time for all β when λ is fixed and β increases, and that z_g advances for a given dispersion time t, and that the mean position of the slug moves faster than the average velocity $\bar{u}$, when the reaction takes place. But it is interesting to note that the displacement of the center of mass (z_g) of the tracer material decreases with increase of λ for a given time and for a fixed β. This is because the decrease in the annular gap contributes to decrease the velocity in the annular pipe (Fig. 2), as well as to increase the inertia of the solute in these region. Aris [2] improved the Taylor's approximation of the effective diffusion coefficient $D_a = \text{Pe}/192 + 1/\text{Pe}$, for asymptotically large time using his method of moments to characterize the tracer distribution. Since the longitudinal diffusion is negligible compared to the lateral diffusion, the effective longitudinal dispersion coefficient D_a can be written as

$$D_a = \frac{1}{2\text{Pe}^2} \frac{d\nu_2}{dt}, \tag{27}$$

where ν_2 is the variance of the longitudinal convective diffusion and D_a represents the interaction between convection and lateral diffusion. For annular flow, D_a is a function of β, λ, and t. The variation of D_a with the dispersion time t and for
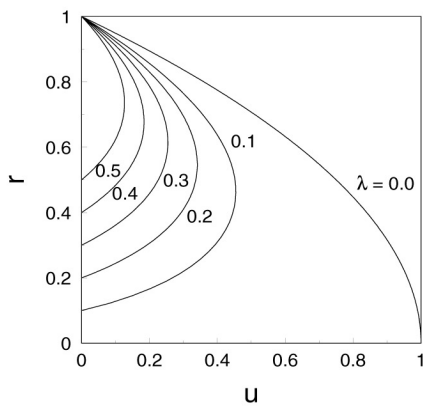
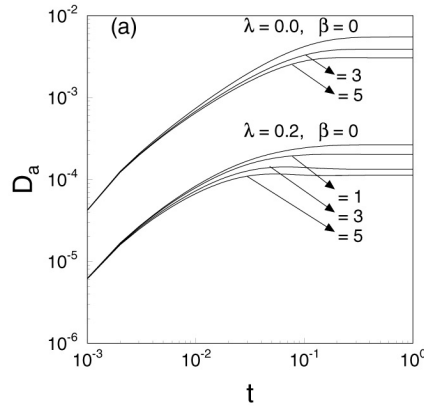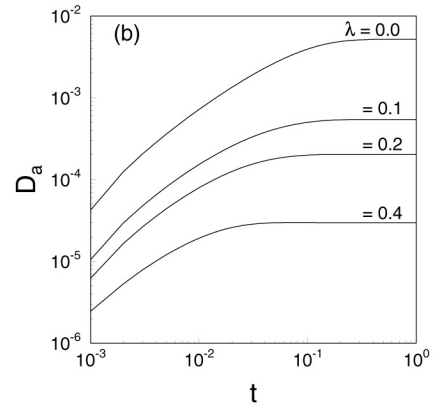**Fig. 2** Velocity profiles for annular flow with various values of the aspect ratio λ.

Fig. 3 Dispersion coefficient D_a for Pe $= 10^3$; (a) $\lambda = 0, 0.2$ for different β; (b) $\beta = 1.0$ for different λ.

Pe $= 10^3$ is presented in Fig. 3a for $\beta = 0, 1, 3, 5$ and $\lambda = 0, 0.2$; in Fig. 3b for $\beta = 1$ and $\lambda = 0, 0.1, 0.2, 0.4$. It is observed that D_a initially increases for small dispersion times t and reaches a steady state for all cases. In Fig. 3a it is observed for $\lambda = 0.2$ and $\beta = 3, 5$ that D_a increases very rapidly for small times t and then decreases slightly before reaching a steady state for large times. It seems that the tracer material is not reduced by the boundary absorption at earlier times. However, the material depletes, when it is absorbed by the pipe boundary. For a given value of λ, D_a decreases with increasing β for all cases. Thus, one would expect from the physical point of view that the increase in absorption at the boundary leads to an increasing number of moles of reactive material undergoing absorption and changes the tracer distribution across the annular pipe, and hence there is a drop in D_a. Fig. 3b shows the variation of the effective dispersion coefficient D_a with time for different values of λ and for fixed β. For all λ, D_a initially increases rapidly and then changes slowly before it reaches a steady state. When the annular gap decreases (i.e. λ increases), D_a reaches a steady state at an earlier time. The decrease in the annular gap leads to a reduction of the dispersion coefficient across the wall, that may be due to the reduction of the flow velocity. It is interesting to note that there is a dimensionless critical time t_c for a fixed β and for an asymptotic steady state of the dispersion coefficient which decreases with increasing λ.

The coefficients of skewness and kurtosis are important criteria to measure the degree of symmetry and peakedness of a concentration distribution of a solute and are defined as

$$\beta_2 = \frac{\nu_3}{\nu_2^{\frac{3}{2}}} \tag{28}$$

and

$$\beta_3 = \frac{\nu_4}{\nu_2^2} - 3. \tag{29}$$

For a Gaussian distribution β_2 and β_3 are zero and the non-zero value of the skewness and kurtosis will indicate deviations from the Gaussian distribution. Fig. 4a–c shows how the skewness is effected by the different Péclet numbers for different
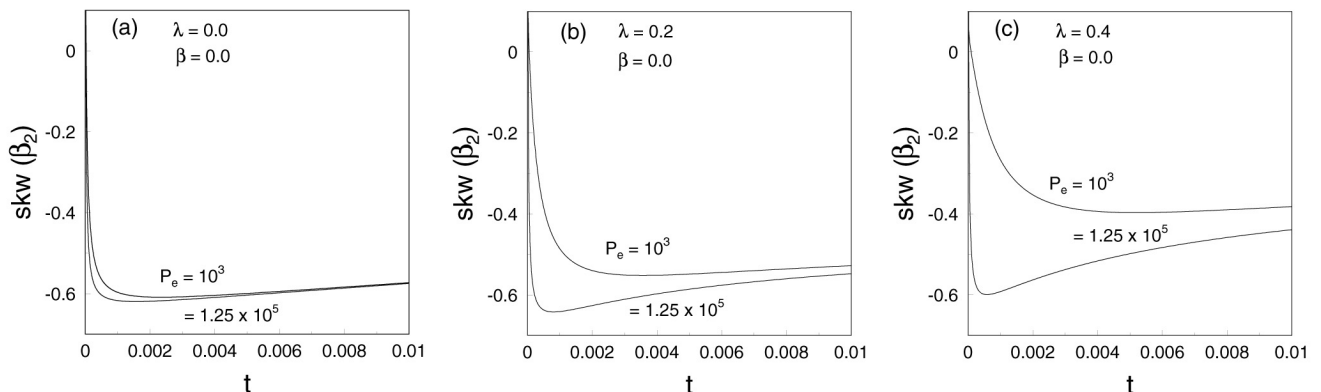

Fig. 4 Skewness β_2 of the distribution for Pe $= 10^3$ and Pe $= 1.25 \times 10^5$; (a) $\lambda = \beta = 0$; (b) $\beta = 0.0$, $\lambda = 0.2$; (c) $\beta = 0.0$, $\lambda = 0.4$.
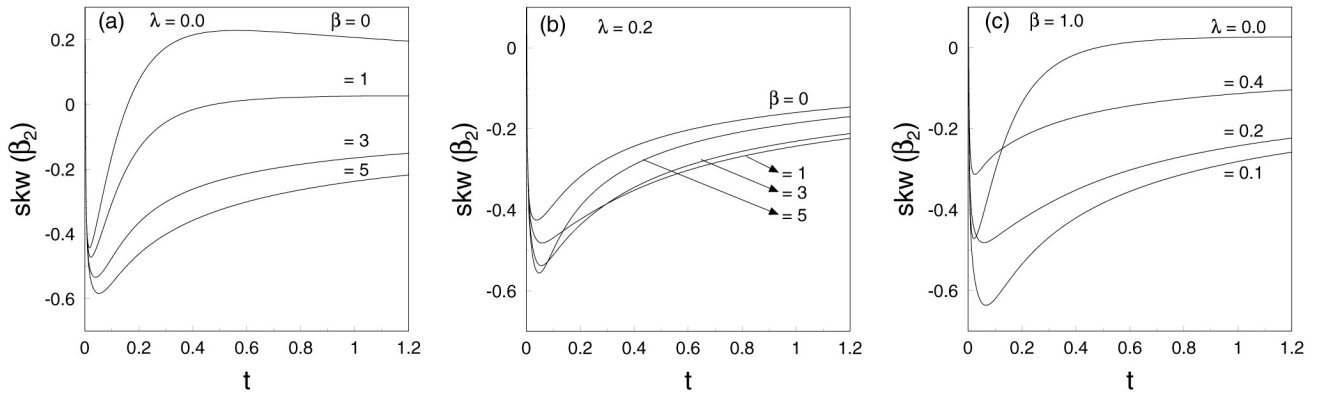
Fig. 5   Skewness β_2 of the distribution for $\mathrm{Pe} = 1.25 \times 10^5$; (a) $\lambda = 0$; (b) $\lambda = 0.2$; (c) $\beta = 1.0$.

values of λ when $\beta = 0$. For $\lambda = \beta = 0$, it is observed that there is no significant change in the skewness with time for $\mathrm{Pe} = 10^3$ and 1.25×10^5, whereas the change in the skewness with increasing λ seems to be significant for these Péclet numbers. Additionally, it is observed that the skewness is independent of Pe for all λ after a certain time. Fig. 5a–c shows the skewness of the concentration distribution for different values of λ and β for $\mathrm{Pe} = 1.25 \times 10^5$ which corresponds to the value of $D = 1/\mathrm{Pe} = 8 \times 10^{-6}$ (Latini and Bernoff [16]). It is interesting to note from the depicted figures that there are significant changes in the dispersion regimes due to changes of the aspect ratio λ and the absorption parameter β at the outer wall. For Poiseuille flow ($\lambda = 0$) in Fig. 5(a), the skewness gradually decreases with increasing reaction parameter β after the diffusive regime ($t = 0.01$); and particularly for $\beta = 1$, the skewness seems to be zero at $t \sim 0.5$, whereas for ($\lambda = 0.2$) in Fig. 5(b) there is some sort of irregularity in skewness within the region $0.01 < t < 0.5$. For large dispersion time t, the skewness tends to zero with increasing absorption parameter β. In Fig. 5(c) for $\beta = 1$, it is seen that the skewness is almost zero for $\lambda = 0$ after a time $t = 0.5$. But for $\beta = 1$ and $\lambda = 0.1$, the skewness decreases abruptly from zero and it tends to zero as λ increases. Perhaps this is due to the asymmetry of the flow for small λ. But as λ increases, the annular flow becomes more symmetric (Fig. 2) and the skewness of the distribution tends to zero for large times. It is interesting to note that the Taylor regime is achieved at $t \sim 0.5$ for Poiseuille flow ($\lambda = 0$) and $\beta = 1$ whereas for annular flow ($\lambda = 0.1$) it is achieved at a later time than the time for Poiseuille flow . Again, as λ increases from 0.1, the skewness tends to zero and the Taylor regime will be reached.

The widely used conventional method of moments provides much information about the concentration distribution across the flow. For any approach to Gaussian distribution, it is worthwhile to use Hermite polynomials with the computed results of higher moments. Once the central moments ν_2, ν_3, ν_4 are known, it is possible to compute the mean concentration distribution $C_m(t, z)$ using the Hermite polynomial representation (Chatwin [4] and Mehta et al. [22]) that is given by

$$C_m(t, z) = M_0(t)e^{-x^2} \sum_{n=0}^{\infty} a_n(t) H_n(x), \tag{30}$$

where $x = \frac{z - z_g}{(2\nu_2)^{1/2}}$, $z_g = \frac{M_1}{M_0}$, and H_i are the Hermite polynomials that satisfy the recurrence relation with $H_0(x) = 1.0$ as

$$H_{i+1}(x) = 2x H_i(x) - 2i H_{i-1}(x), \quad i = 0, 1, 2, \dots \quad . \tag{31}$$

The coefficients a_i are

$$a_0 = 1/(2\pi\nu_2)^{1/2}, \quad a_1 = a_2 = 0, \quad a_3 = 2^{1/2} a_0 \beta_2 / 24, \quad a_4 = a_0 \beta_3 / 96.$$

The variation of the mean concentration distribution $C_m(t, z)$ is presented for various values of λ, $\beta = 0$, and $\mathrm{Pe} = 1.25 \times 10^5$ in Fig. 6(a) for the diffusive regime at $t = 0.8 \times 10^{-4}$, in Fig. 6(b) for the anomalous regime at $t = 0.01$, and in Fig. 6(c) for the Taylor regime at $t = 1.2$. When λ increases, the peak of the distribution increases, the width of the distribution gradually decreases, and the distribution tends to Gaussian distribution (Fig. 6a). In Fig. 6b when $\lambda = 0$, we also have an asymmetric longitudinal distribution for t = 0.01 and as λ increases, the anomaly in the distribution reduces and the width of the distribution becomes gradually smaller with λ. In Fig. 6c, it is observed that the peak of the distribution increases and the width of the distribution decreases as λ increases. In Fig. 7a–c the mean concentration distribution is plotted for an intermediate time $t = 0.05$, for $\mathrm{Pe} = 1.25 \times 10^5$, and for different values of λ and β. In Fig. 7a the distributions for
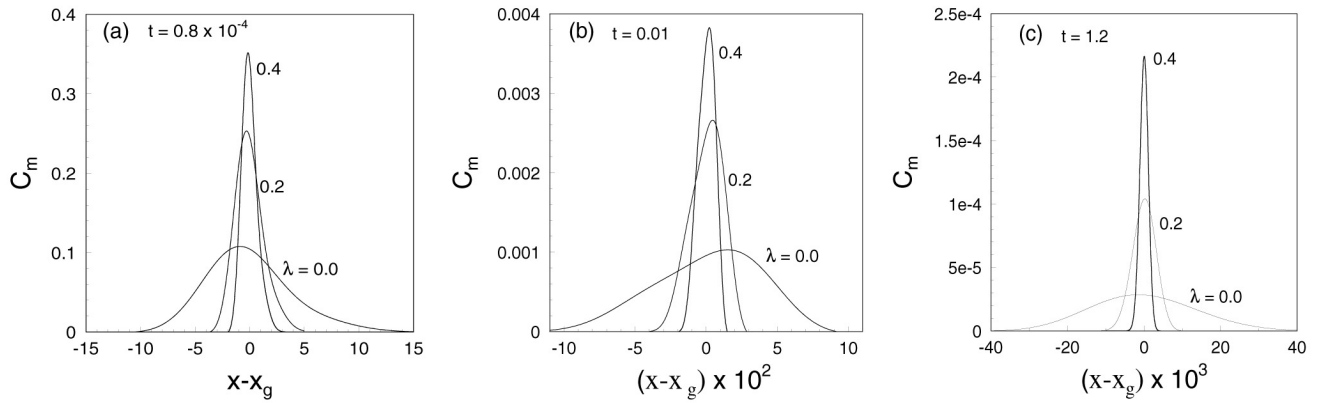
Fig. 6   Mean concentration distribution $C_m(t, z)$ along the pipe for $\beta = 0$, $\mathrm{Pe} = 1.25 \times 10^5$; (a) diffusive regime at $t = 0.8 \times 10^{-4}$; (b) anomalous regime at $t = 0.01$; (c) Taylor regime at $t = 1.2$.
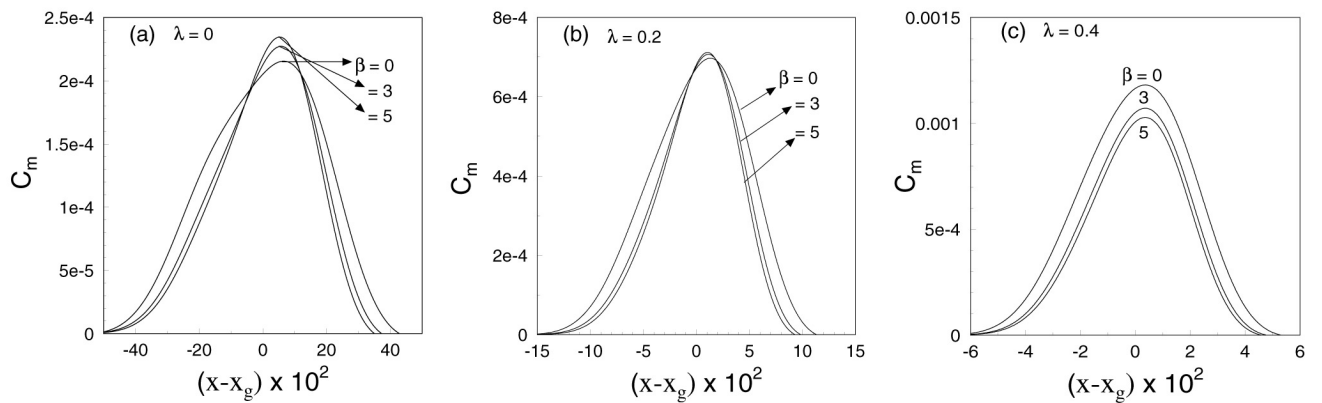

Fig. 7   Mean concentration distribution $C_m(t, z)$ along the pipe for $\mathrm{Pe} = 1.25 \times 10^5$ and the anomalous regime at $t = 0.05$; (a) Poiseuille flow ($\lambda = 0$); (b) $\lambda = 0.2$; (c) $\lambda = 0.4$ for different β.
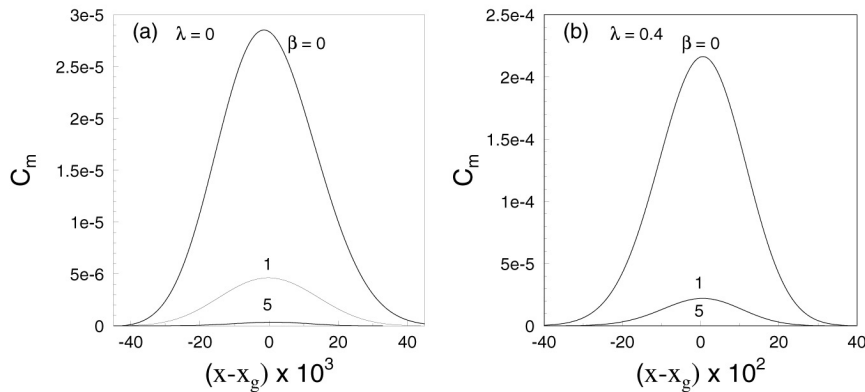

Fig. 8   Mean concentration distribution $C_m(t, z)$ along the pipe for $\mathrm{Pe} = 1.25 \times 10^5$ and the Taylor regime at $t = 1.2$; (a) Poiseuille flow ($\lambda = 0$); (b) annular flow ($\lambda = 0.4$) for different β.

$\lambda = 0$ and $\beta = 0, 3$, and 5 are all asymmetric and as β increases the peak of the distribution increases and tends to the symmetry. In Fig. 7b the distributions for $\lambda = 0.2$ and $\beta = 0, 3$, and 5 are similar to those of $\lambda = 0$ but the effect of the absorption parameter for $\beta = 3$ and 5 is almost the same. In Fig. 7c it is interesting to note that the distribution is almost Gaussian for $\beta = 5$ and the peak of the distribution decreases with increase of the absorption parameter. It can be shown from the figures that there is some anomalous diffusion due to differential convection and boundary absorption observable at the intermediate regime before the Taylor regime. It can be also noticed that the effect of β becomes prominent with an increase of λ. In Fig. 8a,b the mean concentration distribution is plotted only for Taylor's regime at $t = 1.2$ with $\beta = 0, 1$

and 5, $\lambda = 0$ and 0.4, and Pe $= 1.25 \times 10^5$. It is clear that the peak of the distribution gradually decreases as β increases because the total amount of reactive material is reduced due to the absorbing effect of the reaction parameter at the outer wall of the annular pipe. For a fixed β, the tracer distribution in the narrower gap depletes much faster than in the wider gap. The reason for this is that the smaller the annular gap, the larger is the depletion rate of the solute. In the Taylor regime the tracer is completely mixed across the annular pipe diameter and interacts with the absorption boundary, whereas for the diffusive regime it is unchanged due to the effect of the boundary absorption parameter β because the tracer material can not reach the boundary within the short period of interaction. There is only the free-space expansion. A small change in the distribution is observed for the anomalous regime at $t = 0.05$.

5 Conclusion

We have focussed our attention to the dispersion process of the tracer material in an annular flow with boundary absorption, and we have compared some specific results for different aspect ratios with particular emphasis on the role played by the absorbing boundary. A numerical solution of the advection-diffusion equation has been obtained for all time periods, when the solute is injected uniformly over the cross-section of the annular pipe. Due to the effect of the boundary absorption and the aspect ratio, the amount of tracer materials retained in the flow decreases exponentially with dispersion time and the mean longitudinal dispersion of the tracer material decreases with a reduction of the annular gap (i.e. increase of the aspect ratio) for a fixed reaction parameter. The apparent dispersion coefficient D_a increases for small times and asymptotically reaches a steady state for a fixed λ and β. It is important to note that D_a decreases with increasing λ and β, and it can be also seen that the steady state of dispersion is reached at earlier times as λ increases. Therefore, the dimensionless critical time t_c for an asymptotic steady state of the dispersion coefficient reduces with λ. The effect of boundary absorption and the aspect ratio on the mean concentration distribution causes the deviation from the Gaussian distribution. It is interesting to note that the Gaussian distribution (Taylor regime) of the concentration distribution is achieved at $t \sim 0.5$ for Poiseuille flow ($\lambda = 0$) and $\beta = 1$, whereas for annular flow ($\lambda = 0.1$, $\beta = 1$) the Gaussian distribution is achieved at a later time than the time for Poiseuille flow. There is some anomalous diffusion due to the differential convection and the boundary absorption observable at the intermediate regime before the Gaussian distribution is achieved. In the Taylor regime the tracer material is completely mixed across the annular pipe and interacts with the absorbing boundary, whereas in the diffusive regime there is no change in the distribution due to absorption because the tracer material can not interact with the boundary during the short period of time. Small changes are noticed in the anomalous regime.

References

[1] G. I. Taylor, Proc. R. Soc. Lond. A **219**, 186 (1953).
[2] R. Aris, Proc. R. Soc. Lond. A **235**, 67 (1956).
[3] M. J. Lighthill, J. Inst. Math. Appl. (UK) **2**, 97 (1966).
[4] P. C. Chatwin, J. Fluid Mech. **43**, 321 (1970).
[5] W. N. Gill and R. Sankarasubramanian, Proc. R. Soc. Lond. A **316**, 341 (1970).
[6] R. Sankarasubramanian and W. N. Gill, Int. J. Heat Mass Transf. **14**, 905 (1971).
[7] A. R. Rao and K. S. Deshikachar, Z. Angew. Math. Mech. **67**, 189 (1987).
[8] I. Frankel and H. Brenner, J. Fluid Mech. **204**, 97 (1989).
[9] N. A. Stokes and N. G. Barton, J. Fluid Mech. **210**, 201 (1990).
[10] P. S. Gupta and A. S. Gupta, Proc. R. Soc. Lond. A **330**, 59 (1972).
[11] R. Smith, J. Fluid Mech. **134**, 161 (1983).
[12] N. G. Barton, J. Aust. Math. Soc. A, B **25**, 287 (1984).
[13] B. S. Mazumder and S. K. Das, J. Fluid Mech. **239**, 523 (1992).
[14] G. Jayaraman, T. J. Pedley, and A. Goyal, Q. J. Mech. Appl. Math. (UK) **51**(4), 572 (1998).
[15] A. Sarkar and G. Jayaraman, Acta Mech. **158**, 105 (2002).
[16] M. Latini and A. J. Bernoff, J. Fluid Mech. **441**, 399 (2001).
[17] R. B. Bird, W. E. Stewart, and E. N. Lightfoot, Transport Phenomena (John Wiley and Sons, New York, 1960).
[18] H. S. Carslaw and J. C. Jaeger, Conduction of Heat in Solids (Oxford University Press, Oxford, 1959).
[19] D. A. Anderson, J. C. Tanehill, and R. H. Pletcher, Computational Fluid Mechanics and Heat Transfer (Taylor and Francis Inc., London et al., 1997).
[20] N. G. Barton, J. Fluid Mech. **126**, 205 (1983).
[21] A. Mukherjee and B. S. Mazumder, Acta Mech. **74**, 107 (1988).
[22] R. V. Mehta, R. L. Merson, and B. J. Mccoy, J. Chromatogr. **88**, 1 (1974).